ERJ
Engineering Research Journal
Faculty of Engineering
Minoufiya University

MATHEMATICAL AND NUMERICAL MODELING OF UNSTEADY SEDIMENT TRANSPORT UNDER VARIOUS CONDITIONS

Mohammed G. Abd Alla
Irrigation and Hydraulics Dept., Faculty of Engineering, El-Mansoura University

ABSTRACT:
The main goal of this research is to develop one dimensional unsteady and nonequilibrium numerical sediment transport models for alluvial channels. Three mathematical and numerical models have been developed using kinematic, diffusion and dynamic wave approaches for simulating bed profiles in alluvial channels for unsteady and equilibrium conditions. Transient bed profiles were also simulated for several hypothetical cases, comparing different particle velocities and different particle fall velocities. Also different wave models (kinematic, diffusion and dynamic) were compared. The kinematic wave model was developed for simulating transient bed profiles in alluvial channels under unsteady and nonequilibrium conditions and tested with hypothetical data. The diffusion wave model was developed for simulating transient bed profiles in alluvial channels under unsteady, nonuniform and nonequilibrium conditions. It was found that the numerical comparison of kinematic, diffusion and dynamic wave for hypothetical cases of sediment transport revealed under the same sediment flux function of the wavefront is slower in the case of kinematic wave

يهدف هذا البحث إلى تطوير نموذج أحادي الأبعاد لحركة الرسوبيات الغير متزنة والغير مستقرة في القنوات المائية الرسوبيه كما تم أيضا تطوير ثلاثة نماذج رياضية وعددية تحت ظروف تشغيل مختلفة من الحركة والإنتشار ونظريات الأمواج الديناميكية وذلك لمحاكاة التطور في شكل القاع نتيجة للسريان الغير مستقر والمتزنولقد تم أيضا محاكاة التغيرات العابرة في شكل القاع لحالات نظرية إفتراضية مختلفة ومن ثم تم مقارنة سرعات الحبيبات المختلفة وسرعات السقوط للحبيبات ونماذج الأمواج المختلفة (الحركة ، الإنتشار والديناميكي). ولقد تم تطوير نموذج الأمواج الحركي من أجل محاكات أشكال القاع العابرة تحت ظروف السريان الغير مستقر والغير متزن ثم تم استعراض مقارنة ذلك بالبيانات الإفتراضية .

Keywords: Sediment transport, Steady, Unsteady

1. Introduction

The management of soil and water resources is one of the most critical environmental issues facing many countries. For that reason, dams, artificial channels and other water structures have been constructed. Management of these structures encounters fundamental problems: one of them problems is sediment transport.

Sedimentation and soil erosion are some of the modern world's environmental topics. These problems have been studied for centuries by engineers. There are many different approaches for solving these engineering problems. Sediment deposition deals with water and sediment particles so, the physical properties of water and sediment particles should be studied to understand sediment transport mechanism. Sediments are transported as suspended and bed load depending upon fundamental properties of water and sediment particle size, density, etc.

In a river system, loose bed surface can be eroded from a river basin by water and be transported by stream. Sediment particles can be transported in four modes rolling, sliding, saltation and suspension. While sediment particles are sliding and rolling, particles continue to be at contact with the bed. Saltation means jumping motion along the bed in a series of low trajectories. Rolling and sliding particles move along the bed surface under the force of the overlying flow of water. It is often unimportant to distinguish saltation from rolling or sliding because saltation is restricted to a height of only a few grain diameters (Dyer 1986).

A saltating grain may only momentarily leave the bed and rise no higher than a few (<4) grain diameters. These three modes called bed load transport. Sometimes sediments stay in suspension for an appreciable duration called suspended load transport. Suspension of a sediment particle is one of the modes

in water systems that occur when the magnitude of the vertical component of the turbulent velocity is greater than the settling speed of the particle. Bagnold (1966) argued that the major distinction in sediment transport modes is between suspended and unsuspended (bed load) transport.

Bed load sediment grains and aggregates are transported under the combined processes of saltation, rolling, and sliding, and receive insufficient hydrodynamic impulses to overcome gravitational settling. Their only significant upward impulse is derived from successive contacts with the bed (Dyer 1986). When the flow conditions satisfy or exceed the criteria for incipient motion, sediment particles along an alluvial bed will start to move (Yang 1996).

Sediment related disasters such as debris flow, landslides and slope collapses are known to occur naturally, causing social and economic problems in the world. Human civilizations studied sediment transport to reduce the damages of disasters and to maximize the benefits of water resources structures. The studies of the sediment transport can be classified in two categories; physical studies that that are related to extensive flume and field observations. Mathematical studies that are related to the development theoretical and numerical methods.

Physical studies are performed by conducting experiments in laboratory flumes or by taking field observations. It is difficult to represent a river by a laboratory flume; so many assumptions are usually incorporated in laboratory studies. Many investigators have developed empirical methods to represent sediment transport phenomena using data obtained in laboratory, such as Guy, et al. 1966, Langbein and Leopold 1968, Soni 1981, Wathen and Hoey 1998, Lisle, et al. 1997, Lisle, et al. 2001.

To study the sediment transport mechanisms, many investigators developed mathematical equations for real life situations. All the sediment transport mathematical models developed so far are based on five basic physical equations. These equations have been developed by many researches that can be solved both analytically and numerically.

2. Bed Load Transport Formulas

Bed load motion starts when the critical conditions are exceeded. The motion concerns with two phases (solid + liquid) flow near the bed. Generally, the bed load transport rate of a river is about 5-25% of that in suspension. Bed load measurement is difficult, so it is estimated by sediment transport formulas based on different modes of motion employing different parameters, including shear stress and flow velocity. The approaches for predicting bed load are briefly summarized as follows:

2.1 DuBoys Approach

Duboys (1879) developed a bed load model using a shear stress approach. This model consists of sediment particles moving in layers due to the tractive force acting along at the bed. The bed load capacity formula is given as;

$$q_b = K\tau(\tau - \tau_c) \quad (1)$$

where; Straub (1935) defined K as a coefficient that depends on the sediment particle characteristics as:

$$K = \frac{0.173}{d^{3/4}} \quad (2)$$

Thus, DuBoys equation can be rewritten as,

$$q_b = \frac{0.173}{d_s^{3/4}}\tau(\tau - \tau_c) \quad (3)$$

where,
d_s =sediment particle diameter in mm;
τ and τ_c = bed and critical shear stress respectively in Ib/ft^2; and
q_b = bed load transport capacity in (ft^3/sec)/ft.

2.2 Meyer – Peter's Approach

Meyer-Peter et al. (1934) developed the following bed load formula using the energy slope approach in metric system;

$$\frac{0.4q_b^{2/3}}{d_s} = \frac{q^{2/3}S}{d_s} - 17 \quad (4)$$

where,
q_b =bed load [in (kg/s)/m];
q =water discharge [in (kg/s)/m];
S =slope; and
d_s =particle size (in m).

Meyer – Peter formula is valid only for coarse material sediment particle diameters greater than 3 mm. For mixtures of non uniform material, d should be replaced by d 35 , where 35% of the mixture is finer than d 35 (Yang 1996).

2.3 Schoklitsch Formula

Schoklitsch developed two bed load formulas which were developed from discharge approach. The first was published in 1934 in metric units.

$$q_b = 7000\frac{S^{3/2}}{d_s^{1/2}}(q - q_c) \quad (5)$$

where,

q and q_c =water discharge and critical discharge at incipient motion [in m^3/s)/m] respectively
For sand with specific gravity 2.65, critical water discharge can be calculated by plotting for a given flow and grain diameter curve of bed load as ordinate against slope as abscissa and then extrapolating the curve to zero bed load to obtain the intercept with abscissa.

$$q_c = \frac{0.00001944 d_s}{S^{4/3}}$$

(6)

The second bed load formula that was published in 1943 in metric units as:

$$q_b = 2500 S^{3/2}(q - q_c)$$

(7)

2.4 Shields Approach

Shields (1936) conducted laboratory studies and obtained the flow conditions corresponding to incipient motion when sediment transport was greater than zero. Shield's measurements provided semi empirical equation for estimating bed load transport capacity (with English units);

$$\frac{q_b \gamma_s}{q \gamma_w S} = 10 \frac{\tau - \tau_c}{(\gamma_s - \gamma_w) d_s}$$

(8)

2.5 Meyer – Peter and Müller's Approach

Meyer-Peter and Müller (1948) transformed the Meyer-Peter bed load formula by isolating the involved parameters one by one as follows:

$$\gamma \left(\frac{K_s}{K_r}\right)^{3/2} RS = 0.047(\gamma_s - \gamma_w) d + 0.25 \rho^{1/3} q_b^{2/3}$$

(9)

(Ks/Kr) S = the kind of slope which is adjusted for energy loss due to grain resistance, and

$$S = \frac{V^2}{K_s^2 R^{4/3}}$$

(10)

2.6 Regression Approach

Rottner (1959) expressed bed load discharge in terms of the flow parameters based on regression analysis. The formula is dimensionally homogeneous (Yang 1996).

$$q_b = \gamma_s \left[(\zeta_s - 1) g D^3\right]^{1/2} \times \left\{ \frac{V}{\left[(\zeta_s - 1) g D\right]^{1/2}} \left[0.667 \left(\frac{d_{50}}{D}\right)^{2/3} + 0.14 \right] - 0.778 \left(\frac{d_{50}}{D}\right)^{2/3} \right\}^3$$

(11)

where,

ξs =specific gravity of the sediment (=2.65)

2.7 Chang, Simons and Richardson's Approach

Chang, Simons and Richardson (1965) suggested that the bed load discharge by weight can be determined using a shear stress approach;

$$q_b = \frac{K_b \gamma_s V (\tau - \tau_c)}{(\gamma_s - \gamma) \tan \phi}$$

(12)

$$q_b = K_t V (\tau - \tau_c)$$

(13)

Kt = obtained by graph in English unit; and
φ = angle of repose of submerged material

3. Suspended Formulas

Settling velocities are balanced by upward component of turbulent velocity and stays in suspension. While particles fall, some of them are carried away with high flow velocity and then returning near the bed region. Others particles caught in an upward moving eddy are lifted again. The higher the turbulence, the smaller the particle size and the greater the portion of the particles is lifted up. Thus some sediment is kept in suspension. Some basic suspended load approaches are summarized as ***Rouse Equation, Lane and Kalinske's approach, Einstein's approach***.

4. Total Load Transport Formulas

Total sediment load includes both bed load and suspended load. The transported total bed material also consists of bed material load and wash load. However methods for calculating the bed material load and wash load are different. The wash load is estimated by measurements but since the bed surface is changing with incoming flow continuously, it is difficult to predict the wash load in rivers. When comparing the measured and computed total bed load, wash load should be removed from measurements.

5. One Dimensional Hydrodynamic Model

The hydrodynamic model is described by equations of motion in open channel flows. The flow model is developed to solve governing equations based on conservation of mass and momentum. The flow depth and velocity of flow are sufficient to define the flow conditions at a channel cross section, so two governing equations can be solved for a typical flow situation.

In this part, the continuity and momentum equations are derived that are usually referred to as the Saint Venant equations.

5.1 De Saint Venant Equations

The one dimensional modeling of unsteady flow in open channels is most often performed by supplementing de Saint Venant equations that describe the propagation of a wave. In an unsteady modeling, two flow variables, such as the flow depth and velocity or the flow depth and the rate of flow are calculated to define the flow conditions at a channel cross section. Therefore, two governing equations must be used to analyze a typical flow situation. The required equations are the continuity equation and the momentum equation derived with many assumptions (Roberson, et al. 1997, Chaudhry 1993):

- The streamlines do not have sharp curves, so that the pressure distribution is hydrostatic.
- As the channel bottom slope is small, the measured lateral and vertical velocity are approximately same, so the lateral velocity and acceleration component can be neglected.
- No lateral, secondary circulation occurs. The flow velocity distribution is uniform over any channel cross section.
- The channel is prismatic with the same cross section and slope thorough out the distance.
- The head losses in unsteady flow can be simulated by using the steady – state resistance laws, so Chezy and Maning equations can be used also in unsteady flow model. Water has uniform density and flow is generally subcritical (Chaudhry 1993).

5.1.1 Continuity Equation in Unsteady Flows

According to the law of conservation of mass, both the difference of the rate of mass inflow through area dA_1 at section 1 and the rate of mass outflow through area dA_2 at section 2 and the lateral inflow or outflow though Δx in the same time space dt, must be equal to the change of volume.

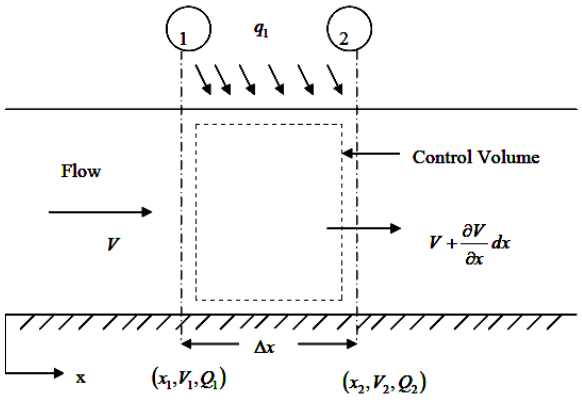

Figure1. *Definition sketch for continuity equation*

So,

$$\frac{\partial M}{\partial t}=\frac{d}{dt}\int_{x_1}^{x_2}\left(\rho A+\rho A_2V_2-\rho A_1V_1-\rho q_1(x_2-x_1)\right)dx=0$$

(14)

where,

M =mass;

A =flow area;

V =flow velocity;

ρ = mass density of water; and

q_1=volumetric rate of lateral inflow or outflow per unit length of the channel between sections 1 and 2. (inflow q_1 is positive, outflow q_1 is negative).

5.1.2 Momentum Equation in Unsteady Flows

The second required equation is derived by considering how the forces on the control volume affect the movement of water through the control volume. The momentum equation states that the rate of change of momentum is equal to the resultant force acting on the control volume as:

$$\sum F=\frac{d(mv)}{dt} \qquad (15)$$

In Figure 2 there is an element which has mass m and length Δx. The rate of changing of total momentum for that element for the uncompressible flows is,

$$\sum F=\frac{d}{dt}\int_{x_1}^{x_2}\left(V\rho A dx+V_2\rho A_2V_2-V_1\rho A_1V_1-V_x\rho q_1(x_2-x_1)\right)\Delta x$$

(16)

where,

Vx =the component of the velocity of lateral inflow in the *x* – direction; and
q_1 = is positive in lateral inflow and negative in lateral outflow.

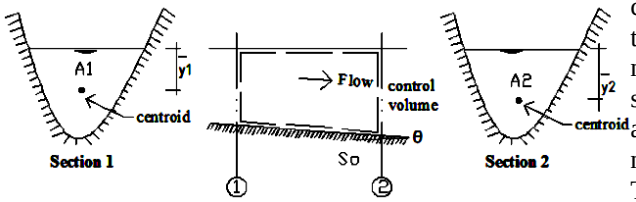

Figure 2. *Definition sketch for momentum equation.*

For steady uniform flow, the friction slope is equal to channel bottom slope. The equation for steady, gradually varied flow is obtained by including the variation of the flow depth and velocity head by including the derivative with respect to distance *x* . The unsteadiness or the local acceleration term is needed to make the equation valid for unsteady nonuniform flow model as:

$$S_f = S_0 \quad -\frac{\partial h}{\partial x} \quad -\frac{\partial}{\partial x}\left(\frac{V^2}{2g}\right) \quad -\frac{1}{g}\frac{\partial V}{\partial t}$$

Steady, uniform — Kinematic Wave Aprox.
Steady, nonuniform — Diffusion Wave Aprox.
Steady, nonuniform — Quasi-Steady Dynamic Wave Aprox.
Unsteady, nonuniform — Full Dynamic Wave Equation

(17)

de Saint Venant equations are nonlinear equations for which numerical methods are required to solve them, so they were not practically applied in their full hydrodynamic form until the 1950s, although they were derived in the early nineteenth century. A number of simplifications were performed by different researchers, being more appropriate in particular situations. Consideration of the implications of the different simplifications can also lead to a better understanding of the full equations, so de Saint Venant equations were described by the propagation of a wave. In wave approximations, the continuity equation is solved simultaneously with the approximate form of the momentum equation. Their differences are all in the momentum equation assumptions. The three types of simplifications for wave models studied in this research are summarized below.

5.2. Kinematic Wave Approximation

The kinematic wave approximation represents the change of flow with distance and time by neglecting the local and convective acceleration terms of the momentum equation. The assumption is that the water surface is parallel to the channel bed (uniform flow assumption) in the kinematic wave approximation. It means there is no way to represent backwater effects. These assumptions reduce the momentum equation to:

$$S_0 = S_f \quad (18)$$

The remaining terms represent the resistance equation for steady, uniform flow as described by Manning's or Chezy's equation but the effects of unsteadiness by an increase or decrease in the flow depth can be taken into consideration.

5.3 Diffusion Wave Approximation

The diffusion wave approximation is a simplified form of the dynamic wave approximation. In addition, it is a significant improvement over the kinematic wave model. In the diffusion wave approach, the *∂h/ ∂t* term from de Saint Venant equation allows the water surface slope to differ from the bed slope. This pressure differential term allows the diffusion model to describe the attenuation of the flood wave. It also allows the specification of a boundary condition at the downstream extremity of the routing reach to account for backwater effects. The simplified form of the momentum equation includes the convective acceleration term representing the spatial change in the flow depth as well as the source terms, but neglects the temporal derivative term as well as the convective acceleration terms due to spatial change in the flow velocity (Chaudhry 1993). The simplified form of the momentum equation is,

$$\frac{\partial h}{\partial x} = (S_0 - S_f) \quad (19)$$

Combining the simplified momentum equation with the continuity equation gives the single equation called the diffusion wave equation.

$$D\frac{\partial^2 Q}{\partial x^2}=\frac{\partial Q}{\partial t}+a\frac{\partial Q}{\partial x}$$

(20)

where,

$$D=Q/2BS_0$$

$$a=dQ/dA$$

5.4 Dynamic Wave Approximation

The dynamic wave equations are the most accurate and comprehensive solution for one dimensional unsteady flow problems in open channels under the specific assumptions. They can be applied to wide range of one dimensional flow problems such as dam break flood wave routing, evaluating flow conditions due to tidal fluctuations, and routing flows through irrigation and canal systems. The full equations can be solved by several numerical methods for incremental times *t* and incremental distances *x* along the water way. The specific terms in the momentum equation are small in comparison to the bed slope. In dynamic wave approximation, the continuity equation is solved simultaneously with the approximate form of the momentum equation. The full dynamic wave approximation can be defined by,

$$\frac{\partial u}{\partial t}+u\frac{\partial u}{\partial x}+g\frac{\partial h}{\partial x}=g(S_0-S_f)$$

(21)

where,

u =the flow velocity (L/T)

h =the flow depth (L)

S f = friction slope

t =independent variable of time (T)

x = independent variable representing the coordinate in the longitudinal direction (flow direction) (L)

6. One Dimensional Sediment Transport Model

The bed of the channel may aggrade or degrade in natural streams if the balance of the water discharge or sediment is destroyed by natural or manmade factors. Eroding loose surfaces from the basin by water deteriorates the ecology and changes the river morphology. The water level rises and brings ecological problems when sediments are deposited in river basins. It is essential to predict the effects of sediment transport for river management. Current research on river sediment transport prediction is mainly based on numerical modeling of sediment transport. One dimensional unsteady sediment transport models were studied in two categories in this research: equilibrium and nonequilibrium.

6.1 One Dimensional Numerical Model for Sediment Transport under Unsteady and Equilibrium Conditions

Bed material transportation is mathematically divided into two independent processes: erosion and deposition. When the erosion and the deposition rates are equal then there is equilibrium. It means that there is no interchange of sediment particles between suspended and bed load sediment transport (Tayfur and Singh 2007). The equilibrium condition exists when the same number of a given type and size of particles are deposited on the bed as are entrained from it. In the literature, most of the studies are based on equilibrium approach although natural rivers are mostly in nonequilibrium state. When flow and sediment discharges, channel geometry and sediment properties do not change substantially for a long period of time, assuming the equilibrium sediment transport conditions is appropriate.

- ***Kinematic Wave Model of Bed Profiles in Alluvial Channels under Equilibrium Conditions***

The kinematic wave model neglects the local acceleration, convective acceleration and pressure terms in the momentum equation for dynamic wave model.

Tayfur and Singh (2006) represented transport movement in wide rectangular alluvial channels as a system involving two layers: water flow layer and movable bed layer, as shown in Figure 3. The water flow layer may contain suspended sediment. The movable bed layer consists of both water and sediment particles, so the movable bed layer includes porosity. The basic one dimensional partial differential equations for unsteady and equilibrium nonuniform transport can be expressed as (Tayfur and Singh 2006):

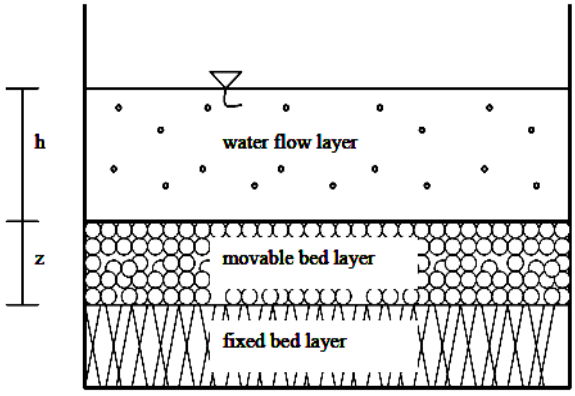

Figure 3. *Definition sketch of two layer system. (After: Tayfur and Singh 2006)*

▪ ***Numerical Solution of Kinematic Wave Equations***

In this model, a finite difference scheme developed by Lax (1954) is used. This scheme can capture shocks, since all the governing equations are solved simultaneously.

There is no need for iterations when gradients are large. The Lax scheme is an explicit scheme and does not require large matrices, so it is easy for solving general empirical equations for roughness and sediment discharge. With reference to the finite difference grid as shown in Figure 4, the partial derivatives and other variables are approximated as follows.

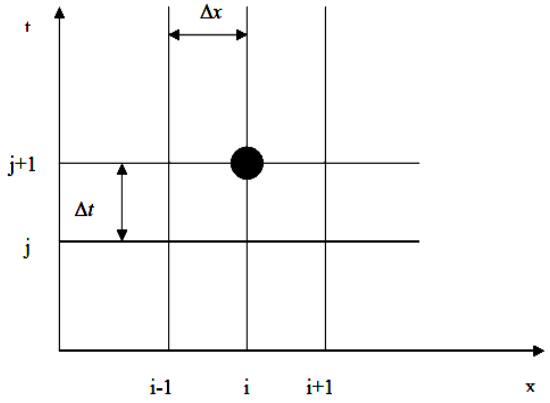

Figure 4. *Finite difference grid*

$$\frac{\partial f}{\partial t} = \frac{f_i^{j+1} - 0.5\left(f_{i+1}^{j} + f_{i-1}^{j}\right)}{\Delta t}$$

$$\frac{\partial f}{\partial x} = \frac{f_{i+1}^{j} - f_{i-1}^{j}}{2\Delta x}$$

(22)

and then,

$$h_i^{j+1} = 0.5(h_{i+1}^{j} + h_{i-1}^{j}) - \frac{\left[1.5\alpha h_{ij}^{\omega} - 1.5\delta\alpha^{*} h_{ij}\right]}{\left[1 - 1.5\delta\alpha^{3} h_{ij}^{0.5}\right]} \frac{\Delta t}{2\Delta x}\left(h_{i+1}^{j} - h_{i-1}^{j}\right)$$

$$- \frac{p}{\left[1 - 1.5\delta\alpha^{3} h_{ij}^{0.5}\right]}\left[z_i^{j+1} - 0.5\left(z_{i+1}^{j} - z_{i-1}^{j}\right)\right]$$

(23)

and,

$$z_i^{j+1} = 0.5(z_{i+1}^{j} + z_{i-1}^{j}) - \frac{\left[2\delta\alpha^{4} h_{ij}\right]}{p} \frac{\Delta t}{2\Delta x}\left(h_{i+1}^{j} - h_{i-1}^{j}\right)$$

$$- \frac{\left[1.5\delta\alpha^{3} h_{ij}^{0.5}\right]}{(1-p)}\left[h_i^{j+1} - 0.5\left(h_{i+1}^{j} - h_{i-1}^{j}\right)\right] - v_s\left[1 - \frac{2z_{ij}}{z_{\max}}\right] \frac{\Delta t}{2\Delta x}\left(z_{i+1}^{j} - z_{i-1}^{j}\right)$$

(24)

Then, the hydrodynamic part of the model is:

$$h_i^{j+1} = 0.5(h_{i+1}^{j} + h_{i-1}^{j}) - \frac{\left[1.5\alpha h_{ij}^{0.5} - 1.5\delta\alpha^{4} h_{ij}\right]}{\left[1 - 1.5\delta\alpha^{3} h_{ij}^{0.5}\right]} \frac{\Delta t}{2\Delta x}\left(h_{i+1}^{j} - h_{i-1}^{j}\right)$$

$$u_i^{j+1} = \alpha\left(h_i^{j+1}\right)^{\beta-1}$$

(25)

The initial conditions can be specified as:

$$h(x,0) = h_o$$

$$z(x,0) = z_o$$

where,

h_0 and z_0= the initial flow depth (L) and the bed level (L), respectively.

The upstream boundary conditions can be specified as inflow hydrograph and inflow sedimentograph.

$$h(0,t) = h(t)$$

$$z(0,t) = z(t)$$

The downstream boundary conditions can be specified as:

$$\frac{\partial h((N,t))}{\partial x} = 0 \qquad (h_{N+1}^{j+1} = h_{N-1}^{j+1}) \qquad t > 0.0$$

$$\frac{\partial z((N,t))}{\partial x} = 0 \qquad (z_{N+1}^{j+1} = z_{N-1}^{j+1}) \qquad t > 0.0$$

▪ ***Model Testing for Hypothetical Cases***

The hypothetical cases were analyzed assuming an inflow hydrograph and sediment concentration at the upstream of the channel, shown in Figures 5a and 5b. The channel was assumed to have a 1000 m length and 20 m width with 0.0025 bed slope. Chezy roughness coefficient is 50 $m^{0.5}$ /sec. The sediment was assumed to have ρ_s= 2650 kg/m^3, d_s = 0.32 mm, p = 0.48 and sediment transport capacity coefficient κ = 0.000075 (Ching and Cheng 1964). Langbein and Leopold (1968) suggested C max = 245 kg/m^2. In Figure 4.3b, C_b = 14 kg/m^2 corresponds the bed level z = 0.01 m and C_b = 140 kg/m^2 corresponds the bed level z = 0.10 m.

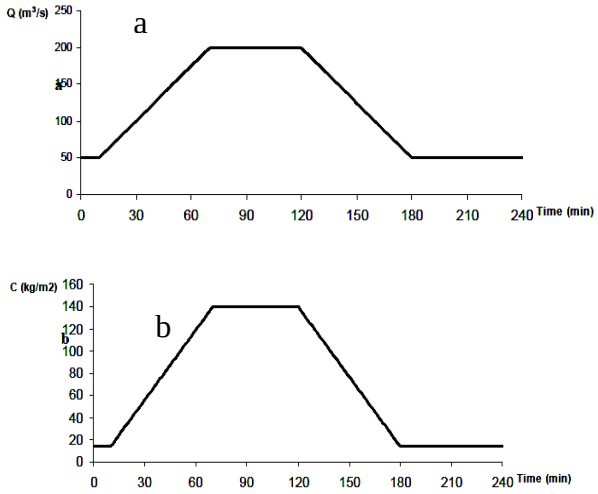

Figure 5. (a) Inflow hydrograph (b) Inflow concentration

- ***Hypothetical Case I: Effect of Inflow Concentration***

Figure 6a shows that when the inflow concentration increases at the upstream end of the channel, bed level gradually increases. In the Figure 6b when the equilibrium feeding of the sediment occurs at the upstream, the bed level continues to increase along the channel length. During the recession limp of the inflow concentration the bed level starts to decrease toward the 10% length of the channel while it increases, toward the 90% length of the channel (**Figure 6c**). Figure 6d shows that the bed level decreases to the original level at the upstream section but as time progresses it increases toward the downstream section.

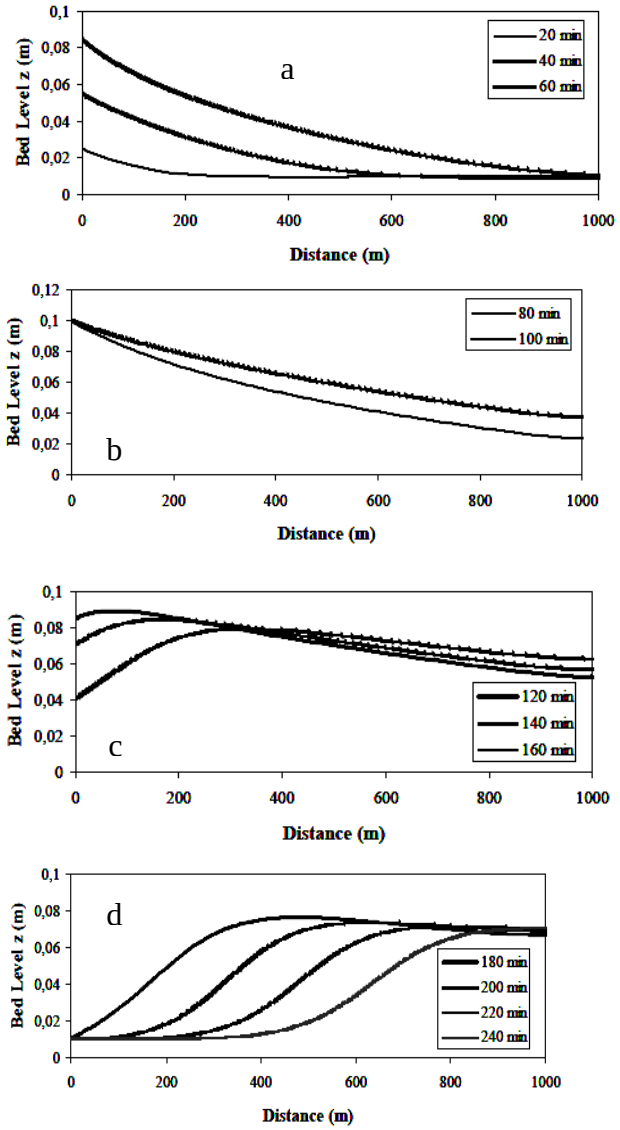

Figure 6. Transient bed profile at (a) rising period (b) equilibrium period (c) recession period (d) post recession period of inflow hydrograph and concentration

- ***Hypothetical Case II: Effect of Particle Velocity and Effect of Particle Fall Velocity***

The objective of this case was to compare the sediment particle velocity and particle fall velocity formulations employed in the developed model. The fall velocity must be obtained for calculating the particle velocity.

In Figures 7a, 7b and 7c it is seen that while Kalinske (1947) and Bridge and Dominic (1984) formula give a faster wavefront, and Chien and Wan (1999) formula give slower wavefront in rising and equilibrium period. At recession period, as the sediment feeding decreases the bed elevation starts to decrease toward the upstream section (in 20% of the channel length) under constant v_s = 0.01 m/s. It is seen that Kalinske (1947) and Bridge and Dominic

(1984) formula give similar performance and sediment moves faster towards downstream end. This is reasonable, since the transient bed profile moves downstream and thus concentration also increases downstream (Figure 7c). In the postrecession period, the bed level increases to original bed level at the upstream section. It is seen that bed profile reached original bed early with Kalinske (1947) and Bridge and Dominic (1984) formula (Figure 7d) (Bor, et al. 2008).

The same simulations were obtained under the other three fall velocity formulations.

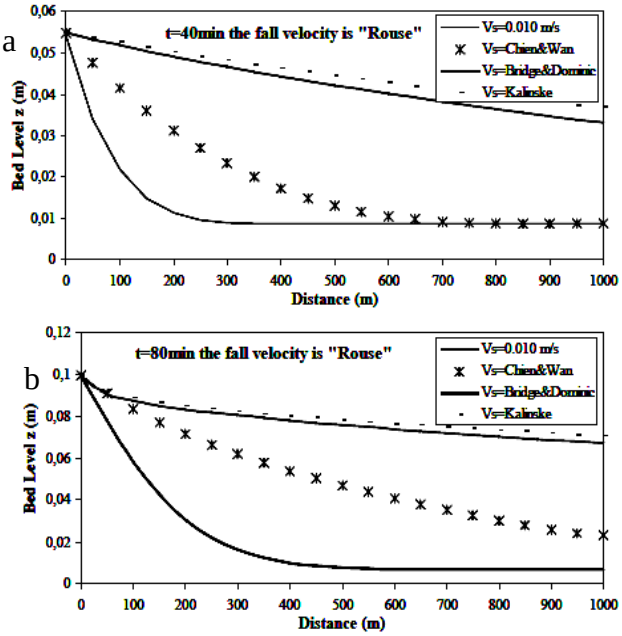

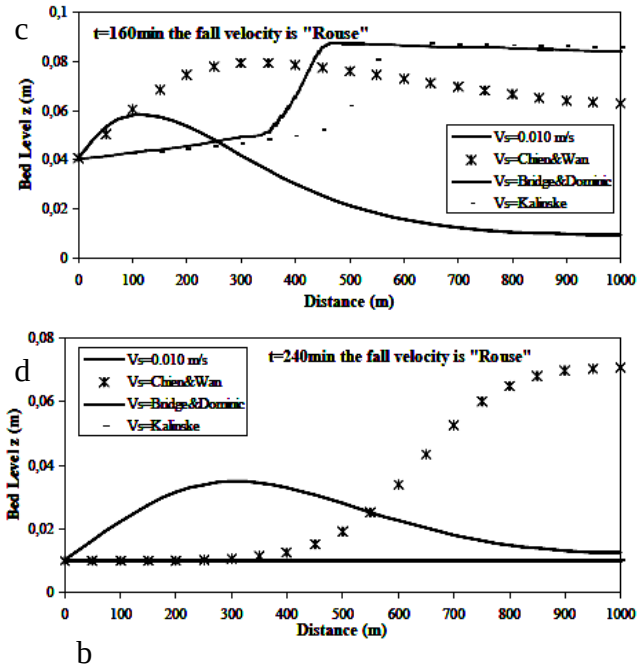

Figure 7. Transient bed profile under different particle velocities at (a) rising period (b) equilibrium period (c) recession period (d) postrecession period of inflow hydrograph and concentration. (After: Rouse 1938, Dietrich 1982, Yang 1996 formula).

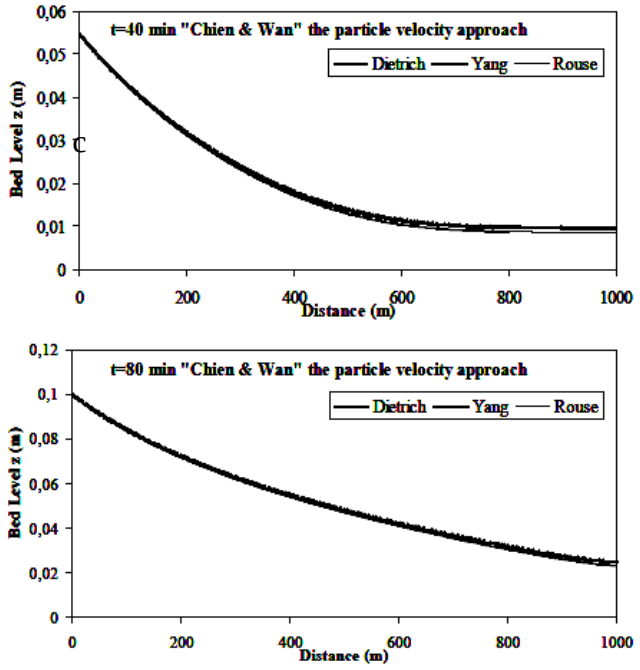

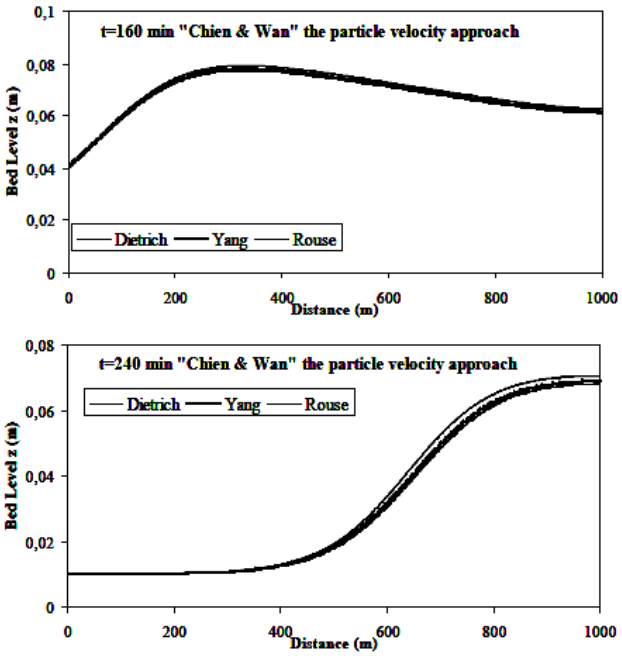

Figure 8. Transient bed profiles under different fall velocities at (a) rising period (b) equilibrium period (c) recession period (d) postrecession period of inflow hydrograph and concentration.

Figures 8a, 8b and 8c demonstrate the effect of the fall velocity on the sediment transport under the different particle velocity formulations is shown. (Rouse 1938) gave nearly the same results under the Bridge and Dominic (1984), Kalinske (1947), and Chien and Wan (1999) particle velocity formulation. For better assessment, the model must be tested with experimented results (Bor, et al. 2008).

The same simulation profiles were obtained under the other three particle velocity formulations.

- ***Model Testing: Comparing the Kinematic, Diffusion and Dynamic Models for Hypothetical Cases***

For the three of wave solutions, a Courant number of 0.2 was selected. The numerical solutions are plotted for $x = 200\ m$, $x = 500\ m$ and $x = 800\ m$ along the channel, respectively (Figure 9 and Figure 10). By comparing Figures 9a, 9b and 9c, one can observe the different behavior of the diffusion and kinematic waves, particularly at peak flow points. The diffusion wave reaches faster to maximum flow rate. On the other hand, the dynamic wave has a smaller peak than the diffusion wave (Figure 5.9a, 5.9b and 5.9c) and kinematic wave has the smallest. It can be said that particle velocity is higher in diffusion and dynamic wave models. Results are acceptable with Kazezyılmaz et al. (2007).

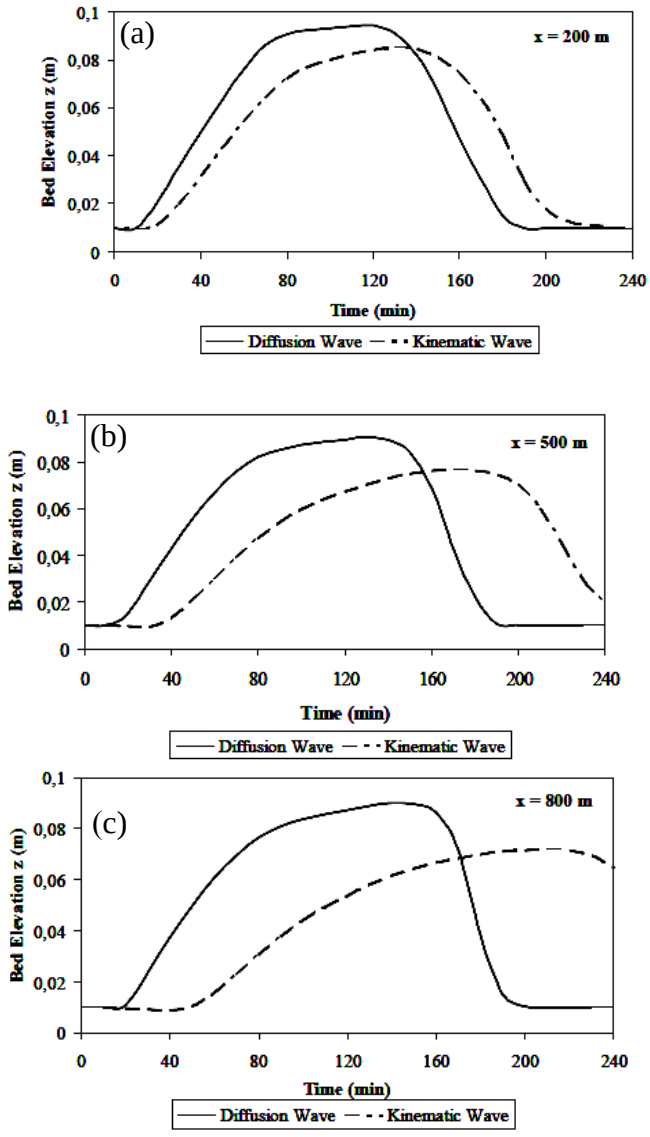

Figure 9. Comparison of numerical solution of Diffusion and Kinematic waves at distance (a) $x = 200\ m$ (b) $x = 500\ m$ (c) $x = 800\ m$ of the channel

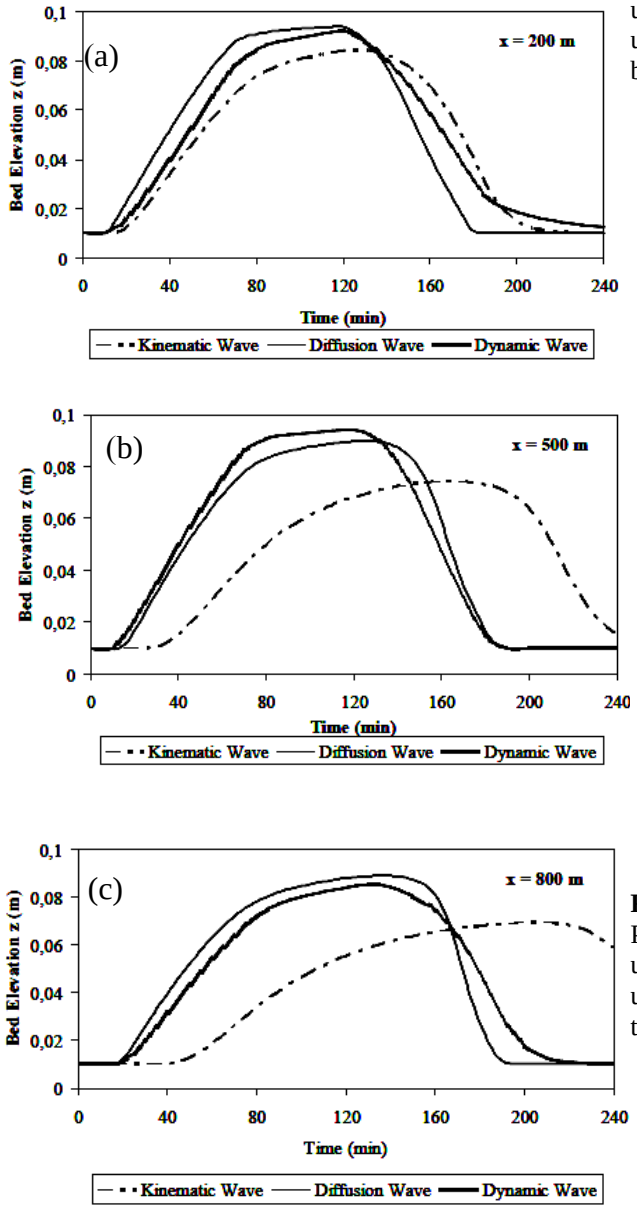

Figure 10. Comparison of numerical solution of Dynamic, Diffusion and Kinematic waves at distance (a) $x = 200\ m$ (b) $x = 500\ m$ (c) $x = 800\ m$ (assuming clear water ($c = 0$)).

- ***Hypothetical Case III: Comparing Three Bed Load Formulas under Kinematic and Diffusion Wave Models***

The objective of this case is to compare the bed load transport formulations employed in the developed model. For that reason, three bed load formulations were selected from the literature. The formulations are Meyer – Peter (1934), Schoklitsch (1934) and Tayfur and Singh (2006) bed load formulations. First of all, the formulations were tested under the kinematic wave model. While Meyer – Peter and Schoklitsch formula gave similar performance, Tayfur and Singh formula gives different performance (Figures 11a and 11b). The sediment particles moved downstream faster under Tayfur and Singh formula. The second test was under the diffusion wave model, where the same behavior was observed (Figures 12a and 12b).

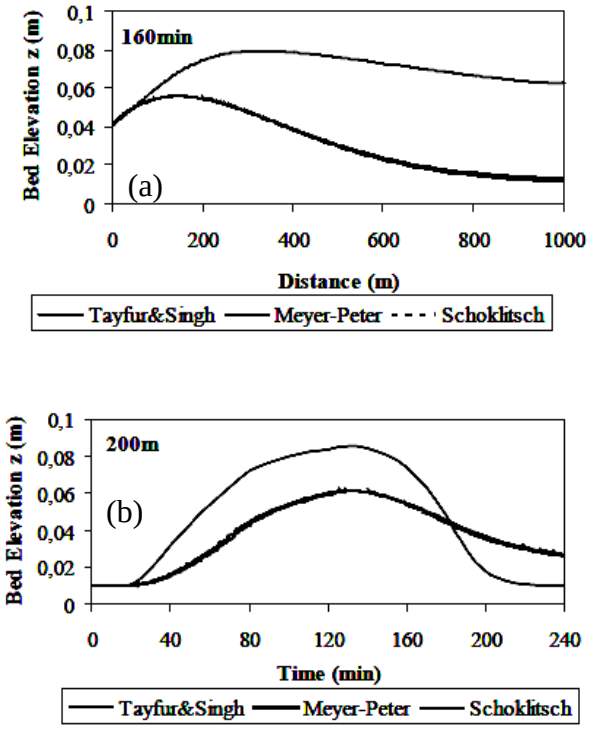

Figure 11. Comparison of Tayfur and Singh, Meyer – Peter and Schoklitsch bed load formulations, (a) under Kinematic wave model at time 160 min. (b) under Kinematic wave model at distance $x = 200m$ of the channel.

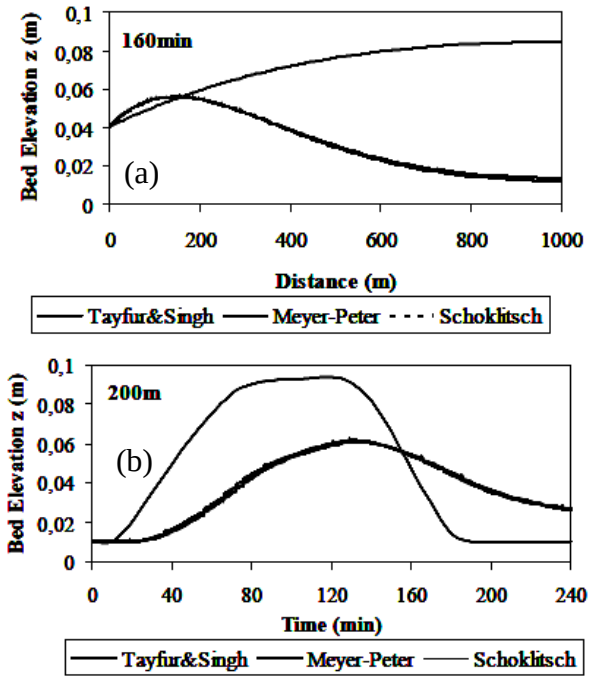

Figure 12. Comparison of Tayfur and Singh, Meyer – Peter and Schoklitsch bed load formulations, (a) under Diffusion wave model at time 160 min. (b) under Diffusion wave model at distance $x = 200m$ of the channel.

It is seen that while Mayer – Peter (1934) and Schoklitsch (1934) formulas gave the same performance, Tayfur and Singh (2006) gives different. Sediment moves faster towards under Tayfur and Singh (2006) formula.

6.2 One Dimensional Numerical Model for Sediment Transport under Unsteady and Nonequilibrium Conditions

All the sediment transport functions or equations presented earlier have been intended for the estimation of bed levels at the equilibrium condition with no scour or deposition, at least from a statistical point of view. It has been assumed that the amount of wash load depends on the supply from the upstream and is not a function of the hydraulic conditions at a given station. Also, the amount of wash load is not high enough to significantly affect the fall velocity of sediment particles, flow viscosity or flow characteristics in a river in comparison with these values in clear water. When the wash load or concentration of fine material is high, non equilibrium bed material sediment transport may occur. The floods may cause heavy erosion and landslides in a river basin causing sediment overloading within a river reach. During the aggradation and degradation process, there may be an exchange of sediment particles between bed layer and suspended layer exceeding the flow capacity. The nonequilibrium sediment transport condition results in an unstable streambed elevation. In such cases, a numerical sediment transport model provides the computational framework for analysis. There are significant differences between the calculations of equilibrium and nonequilibrium conditions. The nonequilibrium condition solution can be obtained by numerical sediment modeling using control volume approach.

- ***Governing Equations***

Tayfur and Singh (2007) studied transport movement in a wide rectangular alluvial channels represented in two layers. Figure 13 shows the possible exchange of sediment between the two layers: the water flow layer and the movable bed layer, depending upon flow transport capacity and sediment rate in suspension.

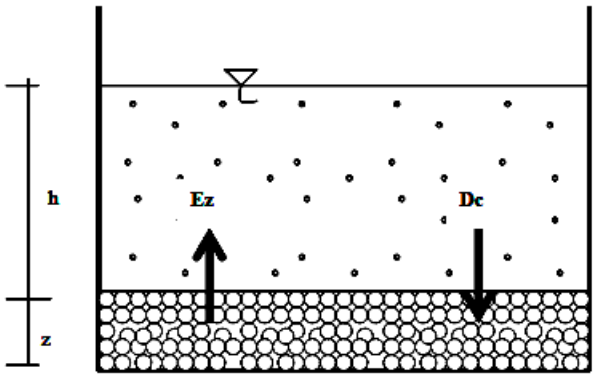

Figure 13. Definition Sketch of two layer system in nonequilibrium condition (After: Tayfur and Singh 2007).

(assuming clear water $c = 0$) and an equation for conservation of suspended sediment in the water flow layer as:

$$\frac{\partial hc}{\partial t}+\frac{\partial huc}{\partial x}=\frac{\partial}{\partial x}\left(V_x h\frac{\partial c}{\partial x}\right)+\frac{v_f}{\eta}\left(c_{eq}-c\right) \quad (26)$$

where,

Vx = the sediment mixing coefficient; and

η = coefficient

The kinematic wave equations for modeling unsteady state, nonuniform transient channel bed profiles under nonequilibrium conditions are:

$$\frac{\partial h}{\partial t}+\alpha\beta h^{\beta-1}\frac{\partial h}{\partial x}+\frac{p}{(1-c)}\frac{\partial z}{\partial t}-\frac{h}{(1-c)}\frac{\partial c}{\partial t}-\frac{\alpha h^{\beta}}{(1-c)}\frac{\partial c}{\partial x}=\frac{q_{1w}}{(1-c)}$$

$$\frac{\partial c}{\partial t}+\alpha h^{\beta-1}\frac{\partial c}{\partial x}+\frac{c}{h}\frac{\partial h}{\partial t}-c\alpha\beta h^{\beta-2}\frac{\partial h}{\partial x}=\frac{q_{1sus}}{h}+\frac{1}{\rho_s h}\left[E_z-D_c\right] \quad (27)$$

$$\frac{\partial z}{\partial t}+v_s\left[1-\frac{2z}{z_{\max}}\right]\frac{\partial z}{\partial x}=\frac{q_{1bed}}{(1-p)}+\frac{1}{\rho_s(1-p)}\left[D_c-E_z\right] \quad (28)$$

For calculating the detachment rate E_z, the shear stress approach was used (Yang 1996);

$$E_z=\sigma T_c=\sigma\left[\Phi(\tau-\tau_{cr})^k\right]$$

$$\tau=\gamma_w h S_o$$

$$\tau_{cr}=\kappa(\gamma_s-\gamma_w)d_s$$

where,

σ = the transfer rate coefficient (1/L);
T = the flow transport capacity (M/L/T);
Φ = the soil erodibility coefficient;
τ = the shear stress (M/L^2);
τ_{cr} = the critical shear stress (M/L^2); and
k = an exponent

- ***Model Application***

The channel was assumed to have a 1000 m length and 30 m width with 0.0015 bed slope.
Chezy roughness coefficient is assumed to be $C_z=36\ m^{0.5}/s$. The sediment was assumed to have $\rho_s = 2650 kg/m^3$, $d_s = 0.32\ mm$ and $p = 0.528$. Maximum concentration was assumed $C_{max} = 500\ kg/m^2$ .Gessler (1965) suggested a value of 0.047 for κ for most flow conditions. The value of transfer rate can be calculated in flumes by $\sigma = 1/(7h)$, where h is flow depth, parameter Φ has a range of 0.0 – 1.0 and exponent k_i has a range of 1.0 – 2.5 in the literature (Foster 1982, Tayfur 2002, Yang 1996). The inflow hydrograph and inflow concentration are given in Figure 14 for upstream boundary conditions.

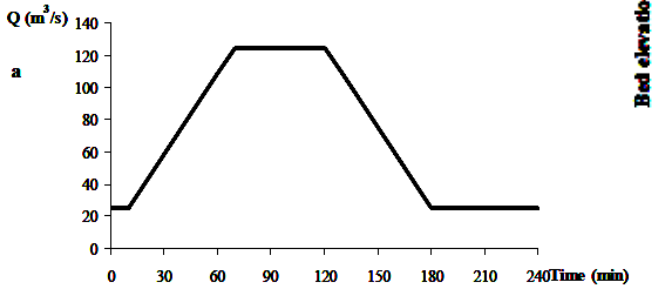

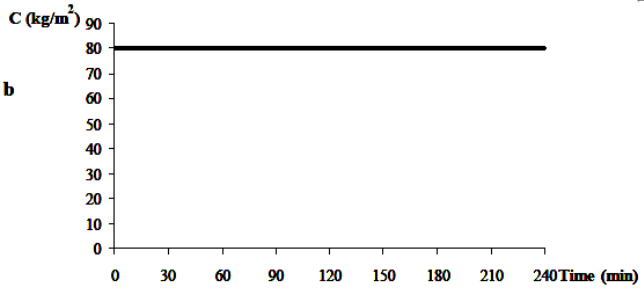

Figure 14. (a) Inflow hydrograph. (b) Inflow concentration.

Figures 15a-15d present bed profiles during the rising limp, equilibrium, recession limb and postrecession limp of the inflow hydrograph and concentration, respectively. It is seen that while inflow concentration increases, the bed level gradually increases in the upstream and it decreases after about 200 m in the downstream (Figure 15a). The bed elevation continues to increase in the equilibrium period at the upstream end (**Figure 15b**).

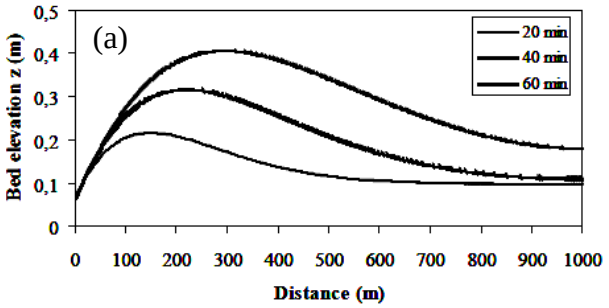

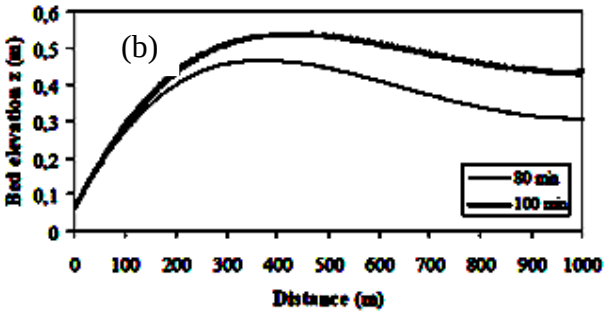

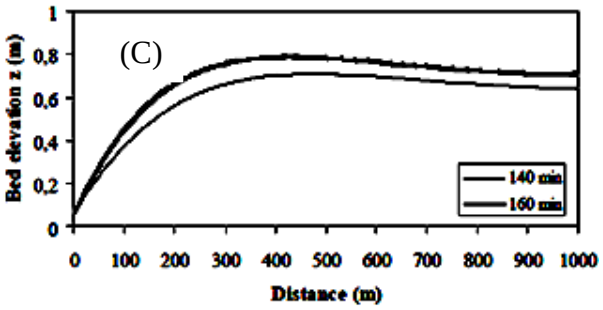

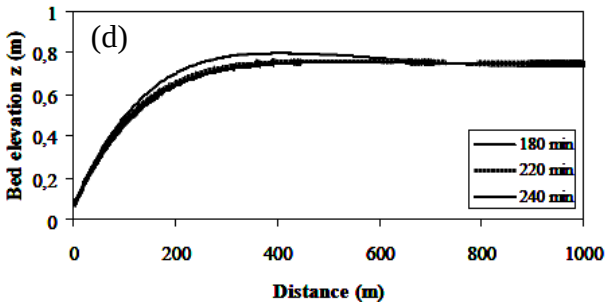

Figure 15. Transient bed profile at (a) rising period (b) equilibrium period (c) recession period (d) post recession period of inflow hydrograph and concentration.

- ***Model Testing: Comparing the Equilibrium and Nonequilibrium models for Hypothetical Cases***

The hypothetical cases were analyzed assuming an inflow concentration hydrograph at the upstream of the channel as shown in Figure 16. The channel was assumed a flume and to have a 20 m length and 1 m width with 0.0001 bed slope.

The sediment was assumed to have ρ_s = 2650 kg/m^3, ds = 0.09 mm, p = 0.45 and sediment transport capacity coefficient κ = 0.000075 (Ching and Cheng 1964). Langbein and Leopold (1968) suggest C_{max} = 500 kg/m^2. The water discharge is $Q = 0.5\ m^3/s$ at the beginning. In equilibrium part $Q = 1\ m^3/s$ (in trapezoidal). For the two model solutions a Courant number of 0.2 was selected. The numerical solutions are plotted for x = 500 m along the channel (Figure 17). It is clear from the figure that the different behavior of the equilibrium and nonequilibrium model, particularly at the peak flow points. The equilibrium model reaches the maximum flow rate faster. On the other hand, the nonequilibrium model has a smaller peak. It can be said that bed material decreases when the suspended sediment increases.

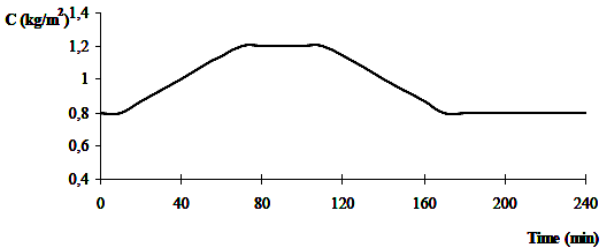

Figure 16. *Inflow concentration*

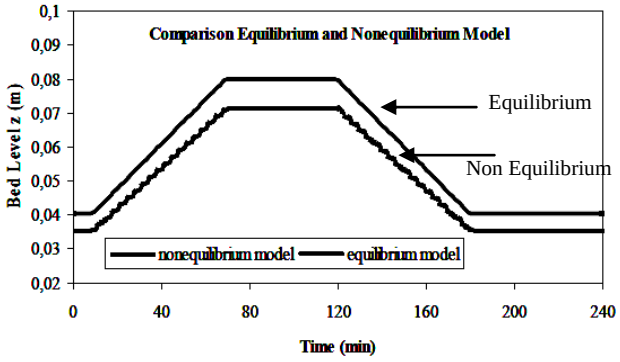

Figure 17. A comparison between the equilibrium and nonequilibrium models

6.3 One Dimensional Numerical Model for Nonuniform Sediment Transport under Unsteady and Nonequilibrium Conditions

One dimensional sediment transport models are simulated in non uniform gravel bed in this section. In this part, the proposed one dimensional model simulates the nonequilibrium sediment transport of nonuniform total load under unsteady flow conditions in rivers. For this reason, de Saint Venant equations are solved for complex materials. The models simulated suspended sediment transport using the nonequilibrium transport approach. In this research, the mathematical model is developed using diffusion wave theory under nonequilibrium condition. The bed profile evolution of complex gravel in alluvial channels is presented in Figure 18.

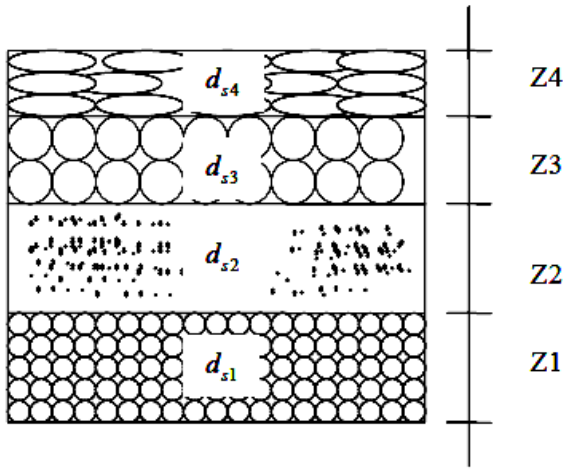

Figure 18.*Multiple – layer model for bed load column*

- ***Governing Equations***

The conservation of mass for suspended sediment in the water flow layer and the conservation of mass for bed sediment in the movable bed layer separately could be written for nonuniform and nonequilibrium sediment transport;

$$\frac{\partial h\sum_{k=1}^{N}c_k}{\partial t}+\frac{\partial hu\sum_{k=1}^{N}c_k}{\partial x}=q_{1sus}+\frac{1}{\rho_s}\left[\sum_{k=1}^{N}E_{zk}-\sum_{k=1}^{N}D_{ck}\right] \quad (29)$$

$$\left(1-\sum_{k=1}^{N}p_k\right)\sum_{k=1}^{N}\left(\frac{\partial z_b}{\partial t}\right)_k+\frac{\partial\sum_{k=1}^{N}q_{bsk}}{\partial x}=q_{1bed}+\frac{1}{\rho_s}\left[\sum_{k=1}^{N}D_{ck}-\sum_{k=1}^{N}E_{zk}\right] \quad (30)$$

where,

C_k = section – averaged sediment concentration of size class k

E_{zk} = the detachment rate of size class k ($M / L^2 /T$)

D_{ck} = the deposition rate of size class k ($M / L^2 /T$)

q_{bsk} = the sediment flux in the movable bed layer of size class k ($L2 /T$)

$(\partial z/\partial t)_k$ = bed change rate corresponding to the k^{th} size class of sediment

P_k = bed material porosity of size class k

- ***Model Application***

The channel is assumed to be as a flume that has 20 m length and 1 m width with 0.0005 bed slope.

Chezy roughness coefficient is assumed to be C_z= 50 $m^{0.5}$ /s. It is assumed that there are four different sediment types in the sediment column. Sediment characteristics used in the model are summarized here in Table 1.

Table 1. *Sediment Characteristics*

type	ρ_s (kg/m^3)	d_s (mm)	p
1	2700	0.5	0.40
2	2650	0.7	0.45
3	2600	0.9	0.55
4	2500	1.2	0.60

maximum concentration of C_{max} = 500 kg / m^2 was assumed for each particle size.

Note that

$$z_{max}=C_{max}/(1-p)\rho_s \quad (31)$$

Gessler (1965) suggested a value of 0.047 for κ for most flow conditions.

The value of transfer rate can be calculated in flumes by $\sigma = 1 / (7h)$, where h is flow depth, parameter Φ has a range of 0.0 – 1.0 and exponent ki has a range of 1.0 – 2.5 in the literature (Foster 1982, Tayfur 2002, Yang 1996). The inflow hydrograph and inflow concentration are given in Figure 19 for the upstream boundary conditions.

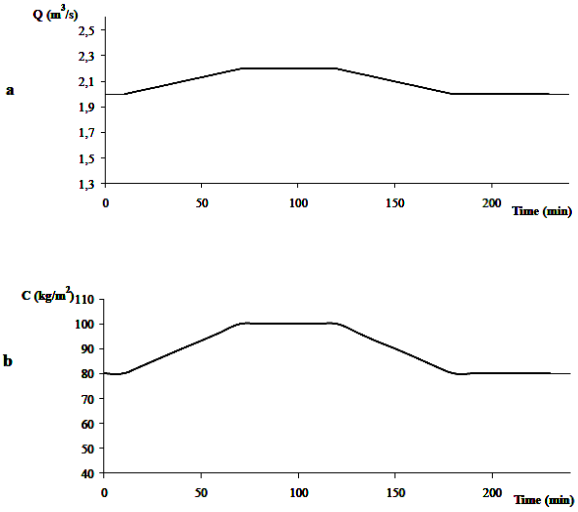

Figure 19. *(a) Inflow hydrograph. (b) Inflow concentration*

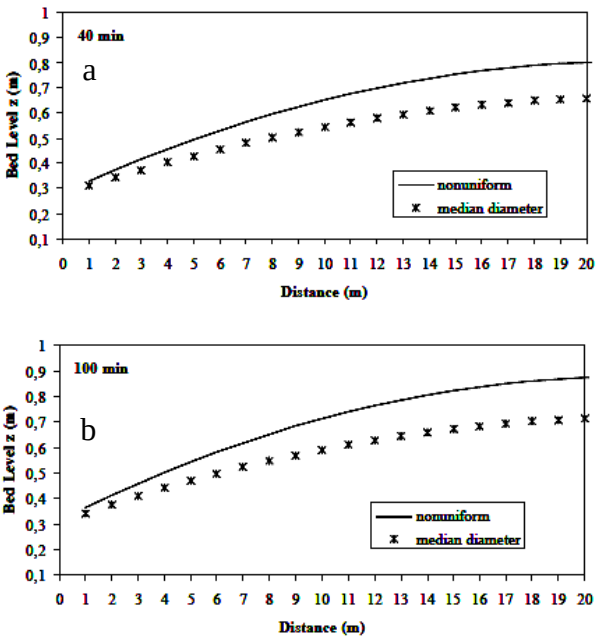

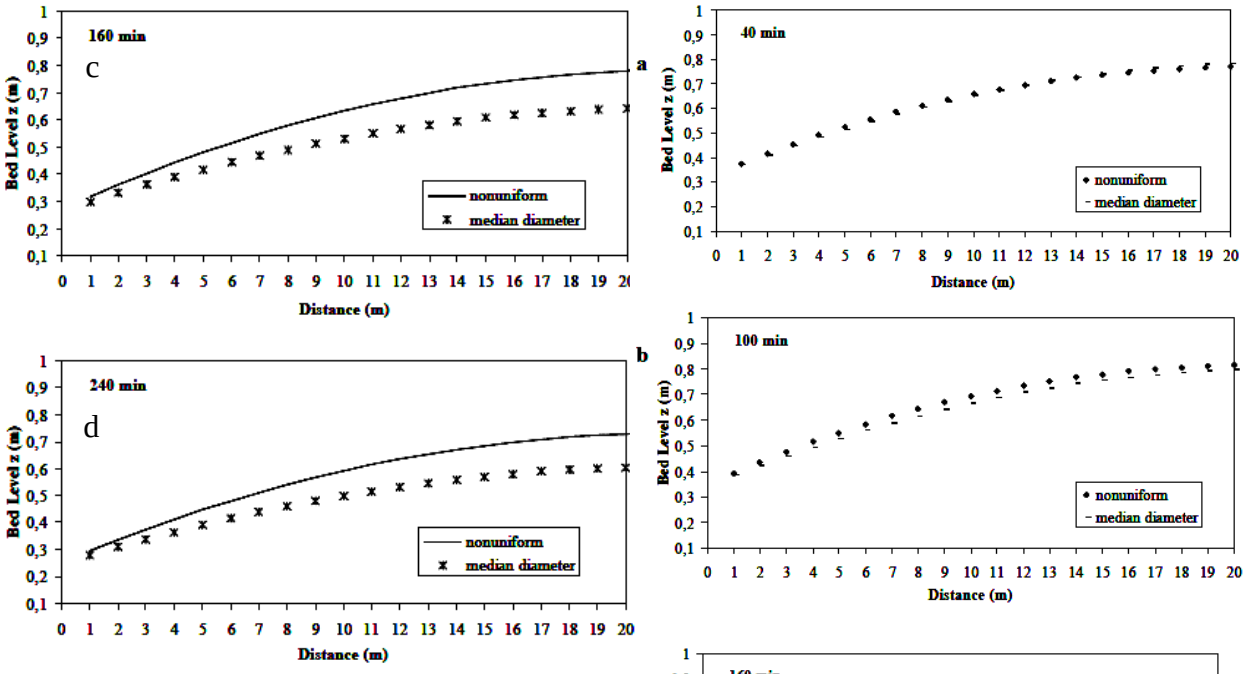

Figure 20. Transient bed profiles of nonuniform sediment and uniform sediment model at (a) rising period (b) equilibrium period (c) recession period (d) post recession period of inflow hydrograph and concentration in unsteady flow conditions.

Simulations were significantly under d_{50} (median diameter) and a nonuniform mixture for all the periods of the simulations. Under $d50$ (median diameter) conditions, bed levels were lower than nonuniform flow case (Figure 20).

In another simulation for the same flume we considered constant inflow hydrograph with Q = 1.2 m^3 / s and the same inflow sedimentograph seen in Figure 19b. The simulations for this case are presented in Figure 21. While nonuniform and uniform sediment transport model give similar performance under steady flow conditions, they have give different performance under unsteady flow conditions (Figure 21).

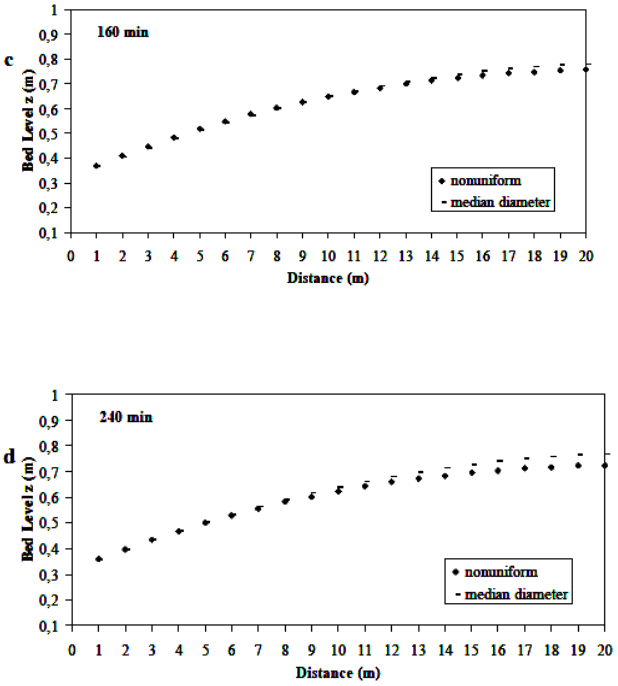

Figure 21. Transient bed profiles of nonuniform sediment and uniform sediment model at (a) rising period (b) equilibrium period (c) recession period (d) post recession period of inflow hydrograph and concentration in steady flow conditions.

7. CONCLUSION

From the study results the following conclusions could be drawn:

1. Numerical model is able to capture the effects of suspended sediment and bed load sediment on sediment transport., otherwise detachment occurs. The model is able to capture this phenomenon of deposition and detachment.

2. The application of the developed model to hypothetical cases revealed that the model is able to capture the behavior of the process in alluvial channels.
3. Modeling the process under nonequilibrium conditions give different results than those under equilibrium conditions. Therefore, if the flow conditions are in nonequilibrium, it should be so modeled.
4. The investigation of different particle velocity formulations revealed that under the same flow conditions, wave front is faster in Kalinske and Bridge and Dominic's formulation.
5. The investigation of different particle fall velocity formulations revealed that under the same flow conditions, they produced nearly the same results.
6. The numerical investigation of different sediment flux (bed load) formulations revealed that under the same transport flow condition, the kinematic wave theory produced different results then Meyer – Peter and Schoklists. Meyer – Peter and Schoklists produced nearly the same profiles. Under kinematic wave theory, the wavefronts move faster.
7. The numerical comparison of kinematic, diffusion and dynamic wave for hypothetical cases of sediment transport revealed under the same sediment flux function of the wavefront is slower in the case of kinematic wave.

REFERENCES

[1] Bagnold, R. A. (1966). An approach to the sediment transport problem from general physics. *Geological survey prof. paper 422-I*. Washington. D.C

[2] Bor, Aslı, Tayfur, G. and Elçi, Ş. (2012). Parçacık Hızı ve Düşüm Hızının Katı Madde Taşınımına Etkisinin Kinematik Dalga Yaklaşımı ile Modellenmesi. *Havza Kirliliği Konferansı*. DSİ II. Bölge Müdürlüğü, Gümüldür, 2008, İzmir: 89-96.

[3] Bridge, J. S. and Dominic, D. F. (1984). Bed Load Grain Velocities and Sediment Transport Rates. *Water Resources Res.* 20(4): 476-490.

[4] Chang, F. M., Simons, D. B. and Richardson, E. V. (1965). Total Bed-Material Discharge in Alluvial Channels. *U.S. Geological Survey Water-Supply* I: 1498.

[5] Chaudhry, M. H. (1993). *Open – Channel Flow*. New Jersey: Prentice Hall, Englewood Cliffs, 07632.

[6] Chien, H. H. and Wan, Z. H. (1999). *Mechanics of Sediment Transport.* Am. Soc. of Civ. Eng. Reston, Va.

[7] Ching, H. H. and Cheng, C. P. (1964). Study of River Bed Degradation and Aggradation by The Method of Characteristics. *Journal of Hydraulic Engineering* 5: 41.

[8]Dietrich, W. E. (1982). Settling Velocity of Natural Particles. *Water Resources Res.*18(6): 1615-1626.

[9] Duboys, M. P. 1879. Le Rhone et les Rivieres a Lit affouillable. *Annales de Ponts et Chausse*, sec. 5, 18: 141-195.

[10] Dyer, K. (1986). *Coastal and Estuarine Sediment Dynamics*. John Wiley & Sons, Inc., New York.

[11] Foster, G. R. (1982). *Modelling the erosion process in hydraulic modeling of small Watersheds.* edited by C. T. Haan, H. P. Johnson, and D. L. Brakensiek. Am. Soc. of. Agric. Eng. St. Joseph. Mich.

[12] Guy, H.P., Simons, D.B., Richardson, E.V. (1966). Summary of alluvial channel data from flume experiments. *Professional Paper 462-I*. United States Geological Society, Washington, D.C.

[13] Kalinske, A. A. (1947). Movement of Sediment as Bed-Load in Rivers. *Transactions of The American Geophysical Union* no:4.

[14] Kazezyılmaz, C. M. and Medina, M. A. (2007). Kinematic and Diffusion Waves: Analytical and Numerical Solutions to Overland and Channel Flow. *J. Hydrologic Eng*. No.2.

[15] Langbein, W. B. and Leopold, L. B. (1968). River channel bars and dunes – Theory of kinematic waves. *Geological survey prof. paper 422-L*. Washington. D.C.

[16] Lax, P. D. (1954). *Weak solutions of Nonlinear Hyperbolic Equations and Their Numerical Computation*. Commun. Pure crnd Appl. Math. 7, 159.

[17]Lisle, T. E., Pizzuto, J. E., Ikeda, H., Iseya, F., and Kodama, Y. (1997). Evolution of a sediment wave in an experimental channel. *Water Resources Research* 33: 1971– 1981.

[18] Meyer-Peter, E., Favre, H. and Einstein, A. (1934). Neuere Versuchsresultate uber den Geschiebetrieb. *Schweiz Bauzeitung* 103(13).

[19] Meyer-Peter, E. and Müller, R. (1948). Formulas for Bed-Load Transport. *International Association of Hydraulic Research. IAHR. 2nd meeting.* Stockholm, Sweden.

[20]Roberson, J.A., Cassidy, J. J. and Chaudhry, M. H. (1997). *Hydraulic Engineering.* 2nd Edition: John Wiley and Sons, Inc. New York, NY.

[21] Rottner, J. (1959). A Formula for Bed-Load Transportation. *LaHouille Blanche* 14(3): 285-307.

[22] Rouse, H. (1938). *Fluid Mechanics for Hydraulic Engineers*. NewYork: Dover.

[23] Shields, A. (1936). *Application of Similarity Principles and Turbulence Research to Bed-Load Movement*. California Institute of Technology. Pasadena.

[24] Soni, J.P. (1981a). Laboratory Study of Aggradation in Alluvial Channels. *Journal of Hydrology* 49: 87-106.

[25]Straub, L. G. (1935). Missouri River Report. *In-House Document 238, 73rd Congress, 2nd Session.*

U.S. Government Printing Office. Washington, D. C. p.1135.
[26] Tayfur, G. (2002). Applicability of Sediment Transport Capacity Models for Nonsteady State Erosion from Steep Slopes. *J. Hydrologic Eng*. 7(3).
[27] Tayfur, G. and Singh, V. P. (2006). Kinematic Wave Model of Bed Profiles in Alluvial Channels. *Water Resour. Res*. 42: W06414.
[28] Tayfur, G., and Singh, V. P. (2007). Kinematic Wave Model For Transient Bed Profiles In Alluvial Channels Under Nonequilibrium Conditions. *Water Resour. Res*. l43: W12412.
[29] Wathen, S. J., and Hoey, T. B. (1998). Morphological controls on the downstream passage of a sediment wave in a gravel bed stream. *Earth Surf. Process Landforms* 23: 715-730.
[30] Yang, C. T. (1996). *Sediment transport: Theory and Practice.* San Francisco: The McGraw-Hill Companies, Inc.